Tokai J Exp Clin Med., Vol. 40, No. 4, pp. 169-177, 2015

Reduced Expression of Hugl1 Contributes to the Progression of Lung Squamous Cell Carcinoma

Tomohiko MATSUZAKI[*1], Susumu TAKEKOSHI[*3], Kentaro TORIUMI[*3], Kanae KITATANI[*3], Madoka NITOU[*1], Naoko IMAMURA[*1], Go OGURA[*2], Ryota MASUDA[*1], Naoya NAKAMURA[*2] and Masayuki IWAZAKI[*1]

[*1]*Division of Thoracic Surgery, Department of Surgery, Tokai University School of Medicine*
[*2]*Department of Pathology, Tokai University School of Medicine*
[*3]*Department of Cell Biology, Division of Host Defense Mechanism, Tokai University School of Medicine*

(Received August 27, 2015; Accepted September 28, 2015)

Cell polarity and cell-cell adhesion play a critical role in the regulation of normal tissue architecture and function. Disruption of cell adhesion and cell polarity is often associated with neoplastic tumors. Loss of apical-basal polarity in epithelial cells is one of the hallmarks of aggressive and invasive cancers. Several polarity proteins including atypical protein kinase C (aPKC), Par6, Par3, and Lethal giant larvae (Lgl, the human homologues of which are called Hugl1 and Hugl2) are localized at the leading edge of migrating cells, and play critical roles during directional migration. Herein, we investigated the expression of aPKC, Par6, Par3, Hugl1, and Hugl2 in lung squamous cell carcinoma (SqCC). An inverse correlation was observed between the expression of Hugl1 and lung SqCC progression. Results of immunohistochemistry and real-time RT-PCR analyses showed that reduced expression of Hugl1 predicts poor survival in lung SqCC patients. The expression of Hugl1 was inversely correlated with both overall survival rate and tumor stage. On the other hand, no associations were observed between the expressions of Hugl2, Par6, and Par3 and lung SqCC progression. These findings indicate that the reduced expression of Hugl1 could be considered as a poor prognostic factor in human lung cancers.

Key words: cell polarity, Lgl1 (Llgl1, Hugl1), lung cancer, squamous cell carcinoma (SqCC), prognostic factor

INTRODUCTION

Lung cancer is the most common cause of cancer death worldwide [1]. Most lung cancers (80%) are classified as non-small cell lung cancers (NSCLC), with majority of the remaining cases (18%) being small cell lung cancers (SCLC) [2]. NSCLC is subdivided into three major histological groups: squamous cell carcinoma (SqCC), adenocarcinoma (AC), and large-cell carcinoma (LCC) [3]. Early-stage NSCLCs are often treated by surgery and radiotherapy, whereas advanced-stage metastatic diseases receive combination chemotherapy. Unfortunately, despite surgical resection and adjuvant therapy, many early-stage NSCLCs relapse and become fatal. The 5-year survival rate for lung cancer is only 60–70% [4], underscoring the need for more effective modalities for the prevention, diagnosis, prognosis, and treatment of this disease [5]. Customized chemotherapy for unresectable or recurrent lung cancers is more frequently used in adenocarcinomas than SqCC [6, 7]. In addition, molecular targeting therapies, including bevacizumab [8, 9], erlotinib [6, 10], and gefitinib [6] have been developed recently. By contrast, there are few therapeutic options for the management of recurrent SqCC. Therefore, it is necessary to examine the histopathological features of SqCC in order to identify the poorest prognostic groups in this cancer. In addition, a thorough understanding of the prognostic factors can help ascertain subsets of patients likely to benefit from certain treatments, or inspire new therapeutic strategies.

Cell polarity and cell-cell adhesion play critical roles in the regulation of normal tissue architecture and function; the disruption of these two characteristics is often associated with neoplastic tumors. Loss of apical-basal polarity in epithelial cells is one of the hallmarks of aggressive and invasive tumors [11]. Several polarity proteins including atypical protein kinase C (aPKC), partitioning-defective proteins (Par3 and Par6), and Lethal giant larvae (Lgl) are localized at the leading edges of migrating cells, and play critical roles during directional migration [12]. In Drosophila, this protein complex localizes within the subapical regions, and is indispensable for the establishment of apical junctions and apical-basal membrane polarity [13–15]. In mammalian epithelial cells, this protein complex localizes at the apical junctions [16–20], and has an important role in the establishment of apical junctions during adhesion-mediated polarization of the epithelial cells [16, 21–25]. An apical protein complex containing aPKC, Par6, and Par3 (Par6-aPKC-Par3 complex), has also been shown to be involved in the establishment of apical-basal polarity in columnar epithelial cells [26–29]. A direct interaction between basolateral Lgl and the apical Par6-aPKC-Par3 complex has been shown in Drosophila and mammalian epithelial cells

Susumu TAKEKOSHI, Department of Cell Biology, Division of Host Defense Mechanism, Tokai University School of Medicine, 143 Shimokasuya, Isehara, Kanagawa 259-1193, Japan Tel: +81-463-93-1121 Fax: +81-463-91-1370 Email: takekos@is.icc.u-tokai.ac.jp

[30–32]. However, the relationship between the formation of the complex and the development of malignant lung cancer remains obscure.

The aPKC isozyme, aPKCλ/ι is overexpressed in several cancers including NSCLC, glioma, and ovarian, colon, breast, gastric, and prostate cancers, and is also thought to be a prognostic factor in several of these tumors [33–37]. *Lgl* is the tumor suppressor gene in Drosophila, the human homologues of which are called *Hugl 1* and *Hugl 2*. Hugl is involved in the regulation of cell polarity and epithelial integrity as well as aPKC. A recent study revealed that reduced expression of Hugl 1 and Hugl 2 has been associated with breast and colorectal cancer progression [38] suggesting that Hugl functions as a tumor suppressor. Reduced expression of Hugl has been implicated in the development of some human cancers [39–42]. The present study demonstrates that reduced expression of Hugl 1 predicts poor survival in lung SqCC. Furthermore, to the best of our knowledge, this is the first study to suggest that decrease in Hugl 1 expression can be considered as a poor prognostic factor in patients with lung SqCC.

MATERIALS AND METHODS

Patients and pathologic data

A total of 103 patients (97 males and 6 females; age range, 43–85 years; mean age, 67.2 ± 9.1 years) with lung SqCC underwent radical surgery (lobectomy and mediastinal lymphadenectomy) at Tokai University Hospital (Kanagawa, Japan). The cancer tissue specimens were obtained from the surgically resected lung SqCC, following receipt of patient's informed consent, according to the Institutional Review Board (IRB No. 11R–002) of Tokai University Hospital. Tumor stages were defined according to the tumor-node-metastasis (TNM) classification, version 7, of the International Union Against Cancer (UICC), while the histological types were defined according to the World Health Organization classifications. The median postoperative follow-up duration was 1,528 (41–3,837) days.

Immunohistochemistry (IHC)

Antibodies were obtained from the following sources and used at the indicated concentrations: anti-aPKCι (BD bioscience, CA, USA), Par 6 (Santa Cruz Biotechnology, CA, USA), Par 3 (Millipore, Billerica, MA, USA), Lgl 1 (Sigma Aldrich, St Louis, USA), and Lgl 2 (Sigma Aldrich). Immunohistochemistry was performed on paraffin-embedded sections of primary tumor and normal lung tissues. Four micrometer-thick paraffin sections were deparaffinized by placing slides into three changes of xylene, and were then rehydrated in a series of graded ethanol. Endogenous peroxidase was inactivated with methanol containing 0.3% hydrogen peroxide for 30 min at room temperature. The samples were rinsed in water and subjected to antigen retrieval at 121℃ for 15min by autoclaving in 1 mM EDTA (pH 8.0) for aPKCι and Lgl 2, in 10 mM citrate buffer (pH 6.0) for Par 6 and Lgl 1, and in antigen retrieval solution (Target Retrieval Solution, pH 9.0, DAKO, Denmark) for Par 3. aPKC, Par 6, Par 3, Lgl 1, and Lgl 2 were detected using the following antibodies in PBS at 4°C overnight: aPKCι(1: 2000 dilution), Par 6 (1: 300 dilution), Par 3 (1: 100 dilution), Lgl 1 (1: 200 dilution), and Lgl 2 (1: 200 dilution), respectively. After washing with PBS, the samples were incubated overnight with anti- rabbit or -mouse secondary antibodies at 4°C. Subsequent to further washes with PBS, horseradish peroxidase activity was visualized using 3'3-diaminobenzidine tetrahydrochloride. The sections were lightly counterstained with hematoxylin. Immunohistochemical specificity of all the antibodies was confirmed by non-immune immunoglobulin PBS.

Evaluation of Immunostaining

The staining intensities of aPKC, Par 6, Par 3, Lgl 1, and Lgl 2 were graded using a semi-quantitative scale from 0 to 2, with 0 = negative, 1 = weak, 2 = strong. In statistical analyses, 0 was defined as negative, whereas 1 and 2 were defined as positive.

Real-time reverse transcription polymerase chain reaction (Real-time RT-PCR)

Tissue sections (four micrometers thick) were prepared from the formalin-fixed, paraffin-embedded tissue blocks and segregated into two groups: normal and tumor. Total RNA was extracted the sections using the RNeasy FFPE Kit (QIAGEN, Hilden, Germany) and reverse transcribed by incubation with random primers using a first-strand cDNA synthesis kit (Applied Biosystems, CA, USA). Real-time RT-PCR was performed by the comparative CT method using TaqMan Universal PCR Master Mix (Applied Biosystems) according to the instructions of the manufacturer, and Hugl 1 and β-actin were quantified using commercially available kits (TaqMan Gene Expression Assays Hs00188098 and Hs99999903, respectively; Applied Biosystems). These primer sets were designed to span one intron to allow for the identification of genomic contamination. The reaction protocol consisted of the following cycles: 95C° for 15 min, 95C° for 15 sec, and 60C° for 1 min for 50 cycles of PCR amplification on an Opticon 2 System (BioRad, CA, USA). All data were analyzed using the Opticon monitor 3 software (BioRad, CA, USA).

Statistical Analysis

Univariate analyses (Chi-square tests, Student's *t*-test, and Dunnett's *t*-test) were primarily used for selecting variables on the basis of a value of $p<0.05$. A Cox proportional hazards regression analysis was used to determine the net effect of each predictor while controlling for the effects of the other factors by univariate and multivariate analyses. Hazard ratios (HR) and their 95% confidence intervals (CI) were used to assess the independent contributions of significant factors. $p<0.05$ was considered to indicate a statistically significant result.

The patient survival time was measured between the date of surgery and mortality from all causes (without discrimination between mortalities resulting from lung carcinoma and other causes). Survival curves were created using the Kaplan-Meier method and compared using the log-rank test. All analyses were performed using the SPSS II statistical software package (version 19.0; SPSS Inc., Tokyo, Japan).

Table 1 Clinicopathological characteristics of the SqCC cases

Age (years)		68 (43-85)
Gender	Male/Female	97/6
Tumor size (mm)		35 (6-95)
Differentiation	Well/moderate/poor	29/61/13
Tumor status	T1a/T1b/T2a/T2b/T3/T4	15/17/37/12/13/7
Nodal metastasis	N0/N1/N2/N3	70/22/11/0
Metastasis	M0/M1a/M1b	101/2/0
Stage	ⅠA/ⅠB/ⅡA/ⅡB/ⅢA/ⅢB/ Ⅳ	25/28/18/10/16/2/2
Lymphatic invasion	Negative/positive	84/19
Venous invasion	Negative/positive	53/50
Observation time (day)		1528 (41-3837)
Reccurrence	Negative/positive	69/34

RESULTS

Patient data

Clinical and histopathological variables are shown in Table 1. The patient group included 97 men and 6 women (age range, 43–85 years; median age, 68 years). The tumors had a median maximum diameter of 35 mm with a range of 6–95 mm. Of the 103 patients, 2 were classified as having stage 0, 25 as stage IA, 28 as stage IB, 18 as stage IIA, 10 as stage IIB, 17 as stage IIIA, 1 as stage IIIB, and 2 as stage IV disease, according to the UICC pathological TNM (pTNM) classification (version 7).

Expression patterns and correlations with clinico-pathological parameters

All markers (aPKC, Par 6, Par 3, Hugl 1, and Hugl 2) investigated by IHC were found to be expressed in the cytoplasm of tumor cells in lung SqCC.

Table 2 depicts the association between the expression of the markers and other clinico-pathological parameters in this study. Univariate analyses revealed that aPKC was associated with lymphatic invasion ($p = 0.029$), tumor stage ($p = 0.036$), and T classification ($p = 0.036$) in univariate analyses, whereas Hugl 1 was found to be associated only with alive/dead ($p = 0.045$). Other markers were not significantly associated with any of the clinico-pathological parameters.

Hugl 1 was localized on the luminal surfaces of bronchial epithelial cells and alveolar cells in non-tumor tissues (Fig. 1A), whereas in tumor tissues, it was found mostly in the cytoplasm and/or plasma membrane of the tumor cells (Fig. 1B and C). However, no associations between localization pattern and histological grade were observed. Fig. 2 illustrates the IHC of human lung SqCC lesions negative or positive for aPKC, Hugl 2, Par 3, Par 6 and Hugl 1. Fig. 3 depicts the Kaplan-Meier survival curves obtained. Overall survival (OS) was longer in the aPKC-negative group than in the aPKC-positive group; however, the correlation between the two was weak ($p = 0.540$; Fig. 3A) because, the majority of the SqCC samples were positive for aPKC. Similarly, weak correlations were observed between lesions negative and positive for the markers Hugl 2, Par 3 and Par 6 (Figs. 3B, C, D). On the other hand, OS was significantly longer in the Hugl 1-positive group when compared to the Hugl 1-negative group ($p = 0.0223$; Fig. 3E).

Quantitative real-time RT-PCR

To determine whether the decrease in Hugl 1 protein expression in progressed human lung SqCC cases was accompanied by the decrease in *Hugl 1* mRNA levels, results from the quantitative real-time RT-PCR analysis for *Hugl 1* mRNA were compared with tumor stage ($n = 32$).

Hugl 1 mRNA levels were found to be correlated with the number of days following surgery, indicating that patients with low *Hugl 1* levels had shorter survival time than those with high levels (Fig. 4A).

Hugl 1 mRNA levels were significantly lower in stage II ($p<0.05$) and stage III ($p<0.01$) tumors when compared with the stage I tumors. Furthermore, *Hugl 1* mRNA levels were significantly lower in stage IIB ($p<0.05$) and stage IIIA ($p<0.05$) when compared with stage IA tumors (Fig. 4B).

Hugl 1/βact mRNA, gender, age, grade and stage were compared with the overall patient survival rate; Hugl 1 expression was found to be a significant prognostic factor ($p = 0.021$) in the cox proportional hazards regression analysis (Table 3).

DISCUSSION

In this study, we have demonstrated that the expression of aPKC and Hugl contributes to the progression of lung SqCC. In particular, the expression of the tumor suppressor gene *Hugl 1* was found to be associated with the prognosis of this disease. IHC and real-time RT-PCR analyses showed that reduced expression of Hugl 1 predicts poor survival in lung SqCC patients. Correlation between Hugl 1 expression and patient survival rate was observed in this study. In addition, an inverse relationship between the expression of Hugl 1 and tumor stage was also noted. These results indicate that Hugl 1 could be considered as a useful prognostic marker in lung SqCC.

Lgl is the tumor suppressor gene in Drosophila, and is associated with cell cycle arrest. The human counterpart, *Hugl*, has significant homology to *Lgl*, and is involved in the regulation of cell polarity and epithelial integrity. [39]. However, it is not clear as to whether the loss of Hugl 1 expression plays a role in human tum-

Table 2 Correlation between cell polarity proteins and clinicopathological parameters of lung SqCC by IHC

Variable	n (%)	aPKC			Par3			Par6			Hugl2			Hugl1		
		negative	positive	χ^2	negative	positive	χ^2	negative	positive	χ^2	negative	positive	χ^2	negative	positive	χ^2
Age at surgery(years)																
<68	50 (48.5)	0	50		4	46		19	31		3	47		10	40	
≧68	53 (51.5)	3	50	0.088	3	50	0.637	19	34	0.821	1	52	0.28	14	39	0.441
Gender																
Male	97 (94.2)	3	94		6	91		36	61		3	94		24	73	
Female	6 (5.8)	0	6	0.662	1	5	0.322	2	4	0.852	1	5	0.095	0	6	0.164
Tumor size (mm)																
≦30	40 (38.8)	2	38		1	39		15	25		1	39		9	31	
>30	63 (61.2)	1	62	0.315	6	57	0.167	23	40	0.919	3	60	0.563	15	48	0.878
Lymph node metastasis																
negative	70 (68.0)	2	68		6	64		27	43		1	69		17	53	
positive	33 (32.0)	1	32	0.961	1	32	0.297	11	22	0.607	3	30	0.06	7	26	0.731
Lymphatic invasion																
negative	84 (81.6)	1	83		7	77		34	50		3	81		21	63	
positive	19 (18.4)	2	17	0.029	0	19	0.192	4	15	0.113	1	18	0.73	3	16	0.391
Venous invasion																
negative	53 (51.5)	0	53		3	50		23	30		2	51		12	41	
positive	50 (48.5)	3	47	0.07	4	46	0.637	15	35	0.159	2	48	0.953	12	38	0.87
Histological differentiation																
Well, Moderate	90 (7.4)	2	88		7	83		36	54		4	86		23	67	
Poor	13 (12.6)	1	12	0.273	0	13	0.298	2	11	0.086	0	13	0.438	1	12	0.154
Stage																
0/Ⅰ/Ⅱ	83 (80.6)	1	82		7	76		30	53		2	81		21	62	
Ⅲ/Ⅳ	20 (19.4)	2	18	0.036	0	20	0.179	8	12	0.748	2	18	0.115	3	17	0.328
T classification																
0/T1/T2	83 (80.6)	1	82		7	76		30	53		3	80		20	63	
T3/T4	20 (19.4)	2	18	0.036	0	20	0.179	8	12	0.748	1	19	0.773	4	16	0.697
M status																
M0	101 (98.1)	3	98		7	94		38	63		4	97		24	77	
M1	2 (1.9)	0	2	0.805	0	2	0.7	0	2	0.275	0	2	0.774	0	2	0.431
Recurrence																
R0	69 (67.0)	2	67		6	63		26	43		2	67		16	53	
R1, R2	34 (33.0)	1	33	0.99	1	33	0.275	12	22	0.813	2	32	0.461	8	26	0.969
alive/dead																
alive	44 (42.7)	2	42		5	39		17	27		1	43		6	38	
dead	59 (57.3)	1	58	0.395	2	57	0.112	21	38	0.752	3	56	0.465	18	41	0.045

origenesis. Recently, reduced expression of Hugl 1 was reported to be associated with the progression of melanomas and breast, colorectal, gastric, hepatocellular, prostate, and ovarian cancers. The *Hugl 1* transcript was reduced or absent in a high proportion of melanomas as well as breast, prostate, and ovarian cancers, indicating its tumor suppressor functions in humans [40]. In colorectal cancer, the loss of Hugl 1 was associated with advanced tumor stage and lymph node metastases in particular [39]. The exclusive presence of aberrant Hugl 1 variants and some truncated Hugl 1 proteins in hepatocellular carcinoma (HCC) and its significant correlations with tumor size and differentiation indicated its use as a potential biomarker for the diagnosis and prognosis of this disease [41]. Furthermore, the loss of Hugl 1 expression plays a role in the development and progression of malignant melanomas [42]. This study demonstrates that reduced expression of Hugl 1 predicts poor survival in lung SqCC. In mammalian epithelial cells, the Par 3-aPKC-Par 6 complex is localized at the apical junctions [16–20] and has an important role in the establishment of these junctions during adhesion-mediated epithelial cell polarization [16, 20–25]. Recent studies have shown physical and functional interactions between Lgl and the apical Par 3-aPKC-Par 6 complex in epithelial cells [43]. Lgl has been shown to be phosphorylated by aPKC, which is required for the process of eliminating Lgl from the apical regions of the epithelial cells. The cell-cell contact initially localizes the "inactive" Par 6-aPKC-Lgl complex in the contact region. Once aPKC is activated, Lgl is phosphorylated and segregated from Par 6-aPKC, forming the "active" Par 3-aPKC-Par 6 complex that promotes the formation of tight junctions (TJ). On the other hand, the segregated Lgl remains in the lateral region and seems to be involved in the establishment of the basolateral membrane [32]. However, it is not known as to whether the complex found in lung SqCC with low Hug1l levels is the "inactive" Par 6-aPKC-Hugl or the "active" Par 3-aPKC-Par 6 form. We have no available materials of lung SqCC to elucidate the phosphorylation statuses of Hugl 1 or the activation status of Par-aPKC-Lgl complex. Further studies will clarify the molecular mechanisms underlying the formation of active or inactive complexes in lung SqCC.

In this study, it was clearly demonstrated that reduced expression of the tumor suppresser gene *Hugl 1* predicts poor survival in patients with lung SqCC. This finding suggests that Hugl 1 is important for the progression of lung SqCC, and might be a novel therapeutic target in these cancers. Furthermore, our results indicated that Hugl 1 may be used as a prognostic

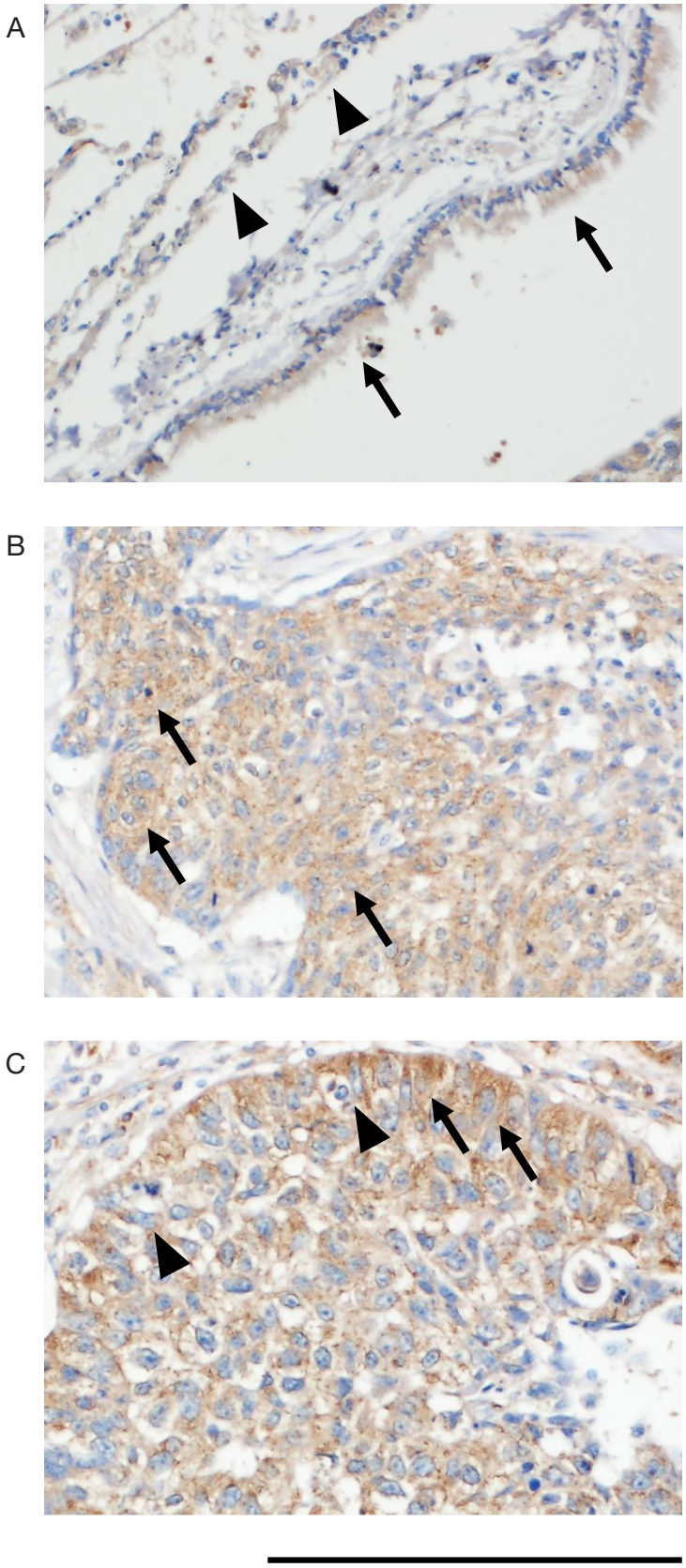

Fig. 1 Representative IHC images demonstrating the localization and distribution of Hugl1 in human lung SqCC (A) and in non-tumor tissue (B). Hugl1 was localized on the luminal surfaces of bronchial epithelial cells (arrow) and alveolar cells (arrowhead) in the tumor tissue (A), whereas in the non-tumor tissue Hugl1 was located within the cytoplasm (arrow; B) and/or the membrane (arrowhead; C) of the tumor cells. Scale bar, 50 μm.

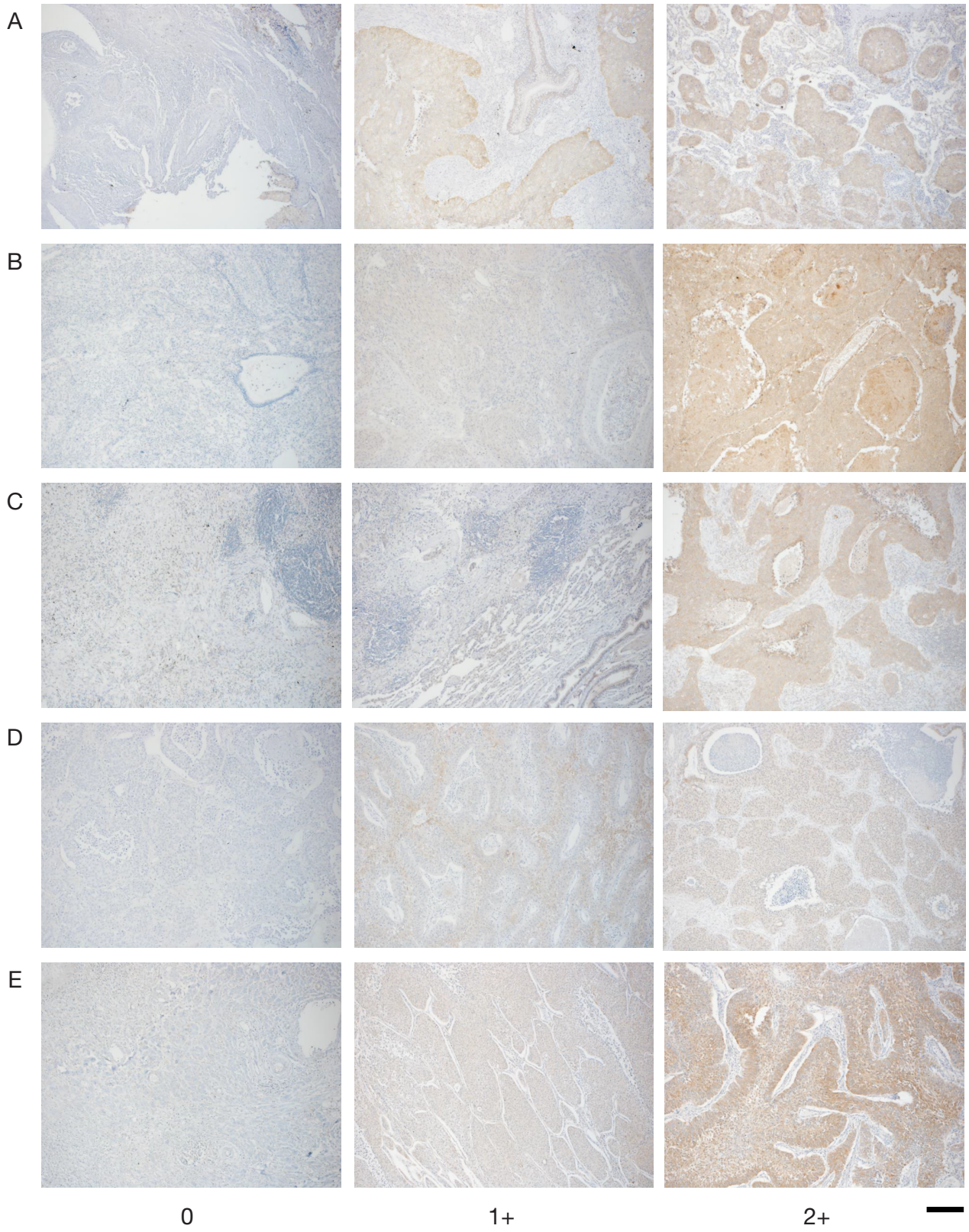

Fig. 2 Micrographs of hematoxylin stained sections of human lung SqCC demonstrating negative (0), slightly positive (1+) and strong positive (2+) reactions for aPKC (A), Hugl2 (B), Par3 (C), Par6 (D) and Hugl1 (E). Scale bar, 50μm.

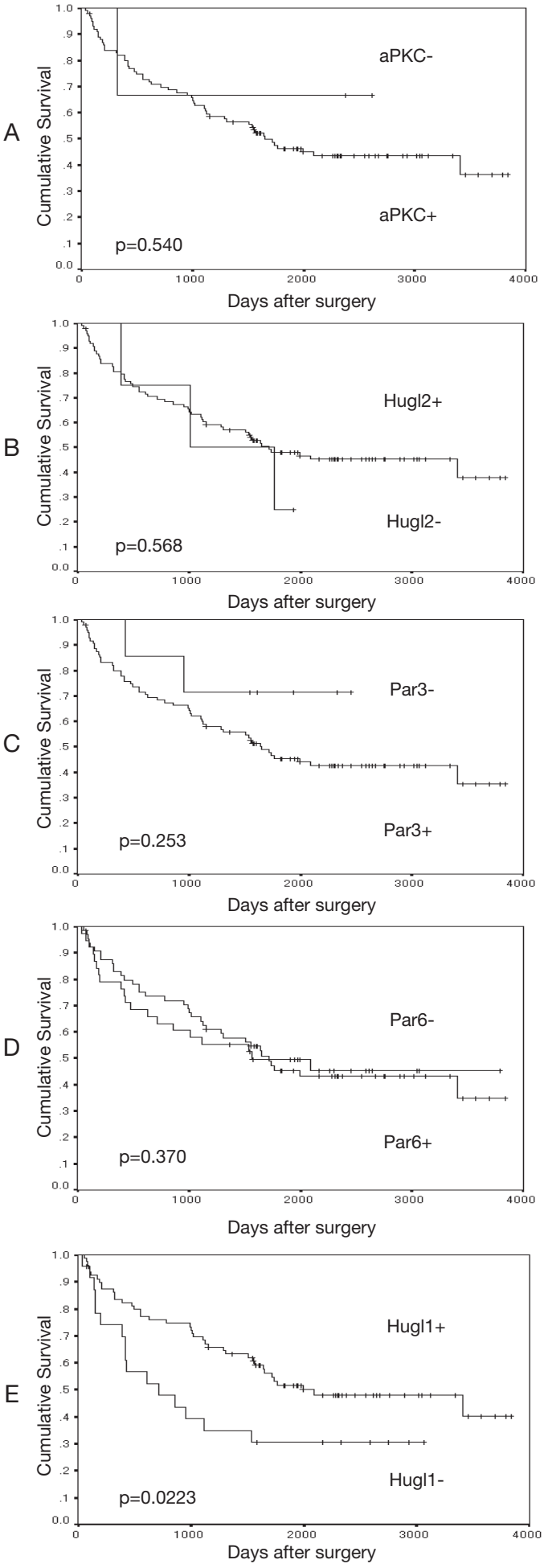

Fig. 3 Kaplan-Meier survival curves in a set of 103 by IHC. The data demonstrating positive and negative expressions for aPKC (A), Hugl2 (B), Par3 (C), Par6 (D), and Hugl1 (E) are shown. No correlations were observed between aPKC ($p = 0.540$), Hugl2 ($p = 0.568$), Par3 ($p = 0.253$), and Par6 ($p = 0.370$) expression status and survival rates. A positive correlation was noted between Hugl1 expression and survival rate ($p = 0.0223$).

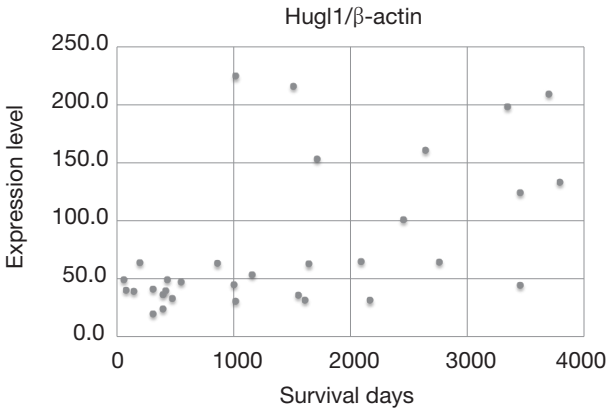

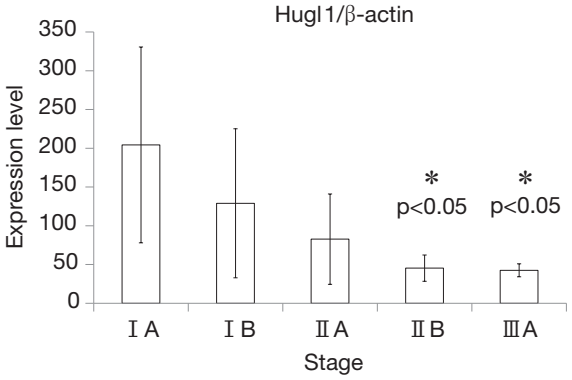

Fig. 4 Graphs demonstrating quantitative real-time RT-PCR analyses for Hugl1/β-actin expression.
(A) *Hugl 1* mRNA levels were found to be correlated with the number of days following surgery, indicating that patients with low *Hugl 1* levels had shorter survival time than those with high levels.
(B) *Hugl 1* mRNA levels were significantly lower in Stage II ($p<0.05$) and stage III ($p<0.01$) tumors when compared with the stage I tumors. Furthermore, *Hugl 1* mRNA levels were significantly lower in Stage IIB ($p<0.05$) and stage IIIA ($p<0.05$) tumors when compared with the stage IA tumors.

Table 3 Cox proportional hazards regression analysis

variable	p-value	Hazard ratio	95% confidence interval
Hugl1/β-actin	0.021	1.005	1.001–1.010
gender	0.020	14.564	1.533–138.337
age	0.009	1.062	1.016–1.111
histological differentiation (well/moderate/poor)	0.443	1.555	0.504–4.798
stage	0.011	0.245	0.082–0.727

marker for clinical diagnosis, lymphatic invasion and metastasis in patients with lung SqCC. Further studies will reveal in more detail the mechanisms by which Hugl1 regulates the progression of these tumors. The findings from this study provide the foundation for generating more effective therapeutic strategies not only in lung SqCC, but in other cancers as well.

ACKNOWLEDGEMENTS

We are grateful to Prof. Hiroyuki Kobayashi for statistical analysis. The authors wish to thank Ms. Makiko Tanaka (Department of Critical Care and Emergency Medicine, Tokai University School of Medicine.), Ms. Yoshiko Itoh, Mr. Johbu Itoh, Ms. Tamaki Sasou, and Mr. Hideo Tsukamoto (Education and Research Support Center, Tokai University School of Medicine) for their technical assistance with immunohistochemical analysis. This work was also supported by a Tokai University School of Medicine Research Aid 2014.

DISCLOSURE/CONFLICTS OF INTEREST

The authors declare no conflicts of interest.

GRANTS

Tokai University School of Medicine Research Aid
Grant-in-Aid for Scientific Research (C) (no. 20590385) from the Japanese Society for the Promotion of Science.

REFERENCES

1) Ferlay J, Shin HR, Bray F, Forman D, Mathers C, Parkin DM. Estimates of worldwide burden of cancer in 2008: GLOBOCAN 2008. International journal of cancer Journal international du cancer 2010; 127: 2893–2917.
2) Schiller JH. Current standards of care in small-cell and non-small-cell lung cancer. Oncology 2001; 61 Suppl 1: 3–13.
3) Beadsmoore CJ, Screaton NJ. Classification, staging and prognosis of lung cancer. European journal of radiology 2003; 45:

8–17.
4) Goldstraw P, Crowley J, Chansky K *et al*. The IASLC Lung Cancer Staging Project: proposals for the revision of the TNM stage groupings in the forthcoming (seventh) edition of the TNM Classification of malignant tumours. Journal of thoracic oncology : official publication of the International Association for the Study of Lung Cancer 2007; 2: 706–714.
5) Parkin DM, Bray F, Ferlay J, Pisani P. Global cancer statistics, 2002. CA: a cancer journal for clinicians 2005; 55: 74–108.
6) Hong J, Kyung SY, Lee SP *et al*. Pemetrexed versus gefitinib versus erlotinib in previously treated patients with non-small cell lung cancer. The Korean journal of internal medicine 2010; 25: 294–300.
7) Rossi A, Ricciardi S, Maione P, de Marinis F, Gridelli C. Pemetrexed in the treatment of advanced non-squamous lung cancer. Lung cancer (Amsterdam, Netherlands) 2009; 66: 141–149.
8) Sandler A, Gray R, Perry MC *et al*. Paclitaxel-carboplatin alone or with bevacizumab for non-small-cell lung cancer. The New England journal of medicine 2006; 355: 2542–2550.
9) Reck M, von Pawel J, Zatloukal P *et al*. Phase III trial of cisplatin plus gemcitabine with either placebo or bevacizumab as first-line therapy for nonsquamous non-small-cell lung cancer: AVAil. Journal of clinical oncology : official journal of the American Society of Clinical Oncology 2009; 27: 1227–1234.
10) Rosell R, Perez-Roca L, Sanchez JJ *et al*. Customized treatment in non-small-cell lung cancer based on EGFR mutations and BRCA1 mRNA expression. PloS one 2009; 4: e5133.
11) Thiery JP. Epithelial-mesenchymal transitions in tumour progression. Nature reviews Cancer 2002; 2: 442–454.
12) Huang L, Muthuswamy SK. Polarity protein alterations in carcinoma: a focus on emerging roles for polarity regulators. Current opinion in genetics & development 2010; 20: 41–50.
13) Muller HA, Wieschaus E. armadillo, bazooka, and stardust are critical for early stages in formation of the zonula adherens and maintenance of the polarized blastoderm epithelium in Drosophila. The Journal of cell biology 1996; 134: 149–163.
14) Petronczki M, Knoblich JA. DmPAR-6 directs epithelial polarity and asymmetric cell division of neuroblasts in Drosophila. Nature cell biology 2001; 3: 43–49.
15) Wodarz A, Ramrath A, Grimm A, Knust E. Drosophila atypical protein kinase C associates with Bazooka and controls polarity of epithelia and neuroblasts. The Journal of cell biology 2000; 150: 1361–1374.
16) Hirose T, Izumi Y, Nagashima Y *et al*. Involvement of ASIP/PAR-3 in the promotion of epithelial tight junction formation. Journal of cell science 2002; 115: 2485–2495.
17) Izumi Y, Hirose T, Tamai Y *et al*. An atypical PKC directly associates and colocalizes at the epithelial tight junction with ASIP, a mammalian homologue of Caenorhabditis elegans polarity protein PAR-3. The Journal of cell biology 1998; 143: 95–106.
18) Joberty G, Petersen C, Gao L, Macara IG. The cell-polarity protein Par6 links Par3 and atypical protein kinase C to Cdc42. Nature cell biology 2000; 2: 531–539.
19) Lin D, Edwards AS, Fawcett JP, Mbamalu G, Scott JD, Pawson T. A mammalian PAR-3-PAR-6 complex implicated in Cdc42/Rac1 and aPKC signalling and cell polarity. Nature cell biology 2000; 2: 540–547.
20) Suzuki A, Yamanaka T, Hirose T *et al*. Atypical protein kinase C is involved in the evolutionarily conserved par protein complex and plays a critical role in establishing epithelia-specific junctional structures. The Journal of cell biology 2001; 152: 1183–1196.
21) Chen X, Macara IG. Par-3 controls tight junction assembly through the Rac exchange factor Tiam1. Nature cell biology 2005; 7: 262–269.
22) Gao L, Joberty G, Macara IG. Assembly of epithelial tight junctions is negatively regulated by Par6. Current biology : CB 2002; 12: 221–225.
23) Mizuno K, Suzuki A, Hirose T *et al*. Self-association of PAR-3-mediated by the conserved N-terminal domain contributes to the development of epithelial tight junctions. The Journal of biological chemistry 2003; 278: 31240–31250.
24) Suzuki A, Ishiyama C, Hashiba K, Shimizu M, Ebnet K, Ohno S. aPKC kinase activity is required for the asymmetric differentiation of the premature junctional complex during epithelial cell polarization. Journal of cell science 2002; 115: 3565–3573.
25) Yamanaka T, Horikoshi Y, Suzuki A *et al*. PAR-6 regulates aPKC activity in a novel way and mediates cell-cell contact-induced formation of the epithelial junctional complex. Genes to cells : devoted to molecular & cellular mechanisms 2001; 6: 721–731.
26) Knust E, Bossinger O. Composition and formation of intercellular junctions in epithelial cells. Science 2002; 298: 1955–1959.
27) Macara IG. Par proteins: partners in polarization. Current biology : CB 2004; 14: R160–162.
28) Bilder D. Epithelial polarity and proliferation control: links from the Drosophila neoplastic tumor suppressors. Genes & development 2004; 18: 1909–1925.
29) Ohno S. Intercellular junctions and cellular polarity: the PAR-aPKC complex, a conserved core cassette playing fundamental roles in cell polarity. Current opinion in cell biology 2001; 13: 641–648.
30) Betschinger J, Mechtler K, Knoblich JA. The Par complex directs asymmetric cell division by phosphorylating the cytoskeletal protein Lgl. Nature 2003; 422: 326–330.
31) Hutterer A, Betschinger J, Petronczki M, Knoblich JA. Sequential roles of Cdc42, Par-6, aPKC, and Lgl in the establishment of epithelial polarity during Drosophila embryogenesis. Developmental cell 2004; 6: 845–854.
32) Yamanaka T, Horikoshi Y, Sugiyama Y *et al*. Mammalian Lgl forms a protein complex with PAR-6 and aPKC independently of PAR-3 to regulate epithelial cell polarity. Current biology : CB 2003; 13: 734–743.
33) Ishiguro H, Akimoto K, Nagashima Y *et al*. Coexpression of aPKClambda/iota and IL-6 in prostate cancer tissue correlates with biochemical recurrence. Cancer science 2011; 102: 1576–1581.
34) Kojima Y, Akimoto K, Nagashima Y *et al*. The overexpression and altered localization of the atypical protein kinase C lambda/iota in breast cancer correlates with the pathologic type of these tumors. Human pathology 2008; 39: 824–831.
35) Regala RP, Weems C, Jamieson L *et al*. Atypical protein kinase C iota is an oncogene in human non-small cell lung cancer. Cancer research 2005; 65: 8905–8911.
36) Takagawa R, Akimoto K, Ichikawa Y *et al*. High expression of atypical protein kinase C lambda/iota in gastric cancer as a prognostic factor for recurrence. Annals of surgical oncology 2010; 17: 81–88.
37) Mandil R, Ashkenazi E, Blass M *et al*. Protein kinase Calpha and protein kinase Cdelta play opposite roles in the proliferation and apoptosis of glioma cells. Cancer research 2001; 61: 4612–4619.
38) Spaderna S, Schmalhofer O, Wahlbuhl M *et al*. The transcriptional repressor ZEB1 promotes metastasis and loss of cell polarity in cancer. Cancer research 2008; 68: 537–544.
39) Schimanski CC, Schmitz G, Kashyap A *et al*. Reduced expression of Hugl-1, the human homologue of Drosophila tumour suppressor gene lgl, contributes to progression of colorectal cancer. Oncogene 2005; 24: 3100–3109.
40) Grifoni D, Garoia F, Schimanski CC *et al*. The human protein Hugl-1 substitutes for Drosophila lethal giant larvae tumour suppressor function in vivo. Oncogene 2004; 23: 8688–8694.
41) Lu X, Feng X, Man X *et al*. Aberrant splicing of Hugl-1 is associated with hepatocellular carcinoma progression. Clinical cancer research : an official journal of the American Association for Cancer Research 2009; 15: 3287–3296.
42) Kuphal S, Wallner S, Schimanski CC *et al*. Expression of Hugl-1 is strongly reduced in malignant melanoma. Oncogene 2006; 25: 103–110.
43) Yamanaka T, Horikoshi Y, Izumi N, Suzuki A, Mizuno K, Ohno S. Lgl mediates apical domain disassembly by suppressing the PAR-3-aPKC-PAR-6 complex to orient apical membrane polarity. Journal of cell science 2006; 119: 2107–2118.